An intuitive interface for null space visualization and control of redundant surgical robots

M. Karnam[1*], R. Parini[1], M. Eugster[1], P. Cattin[2], G. Rauter[1], and N. Gerig[1]

[1] BIROMED-Lab, [2] CIAN

Department of Biomedical Engineering, University of Basel, Basel, Switzerland

[*] Corresponding author, email: murali.karnam@unibas.ch

Abstract: Surgery robots used to position instruments maybe redundant and therefore have null space movements which allows changing the robot's shape without changing the desired end-effector pose. However, null space movements are often not intuitive and challenging to predict for human operators. We propose a simple interface to visualize possible null space based on a user input using force/torque sensor. The interface was implemented and tested successfully for a 7-degrees-of-freedom KUKA LBR iiwa robot. This interface was designed for any medical personnel to preview possible robot's shapes and select a favorable one while the main surgeon independently teleoperates the end-effector pose.

I. Introduction

Robots in operating rooms are mostly used in tele-operation mode, where a surgeon controls the movement of instruments mounted on a robot using an interface. Surgical robots have the advantage of realizing accurate movements beyond human capabilities, and tele-operation gives complete robot control to the surgeon. Robots can be designed specifically for one type of surgery such as the Mako (Stryker, USA), or general purpose robots can be used, such as the KUKA LBR Med (KUKA, Germany) used for Laserosteotomy [1].

Robots can have redundant degrees of freedom (DoF), meaning they have more controllable DoF than needed for the desired task. These additional DoF form the null space and can be used to control the shape of the robot, while the pose of the end-effector remains fixed. The null space allows robots to move around obstacles, such as medical equipment, or get out of surgical personnel's working area, while the end-effector, e.g. an endoscope can keep its pose. However, controlling the shape of the robot in null space may be not intuitive via teleoperation, and therefore, challenging to predict and control for a human operator.

Different strategies are available for controlling the redundant DoF of robots while they perform trajectory tracking. For example, priority-based controllers find an appropriate set of joint velocities (or torques) attributing highest priority to the desired end-effector pose and lower priority to control the null space velocity without hampering the pose [2, 3]. Such techniques are also used in surgical scenarios, e.g., force input by the surgeon on the elbow of a robot reshapes the robot in null space [4]. Similar strategies are applied to respect additional constraints, such as to incorporate a remote center of motion (RCM) as additional higher priority tasks [5]. However, in all scenarios, the robot's shape change maybe different than desired and hard to predict.

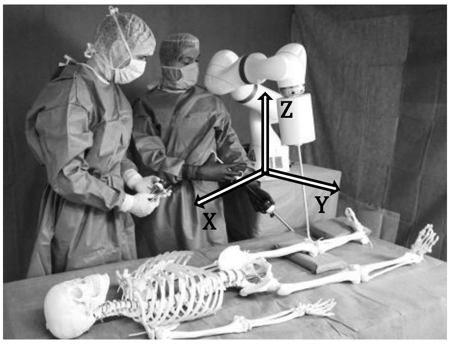

Figure 1: A robotic surgery mock-up where the robot interferes with the surgeon's workspace. The objective of this work is to equip the user with an interface to visualize alternative robot configurations with the same end-effector pose.

In a typical surgical scenario, physicians work in vicinity to the robot. Therefore, the robot should be reshaped when it occupies a workspace that is needed otherwise (Fig. 1). Here, we offer a novel user interface enabling the medical personnel to visualize different possible robot configurations for a given end-effector pose and select the most suitable one. This interface can be used by the medical personnel independently of the surgeon who performs the intervention through teleoperation. This is only possible since the robot's null space (shape) can be controlled independently of the robot's end-effector pose.

II. Material and methods

In this work, a 7-DoF KUKA LBR iiwa is used for a 6-DoF task to control the pose of an endoscope. It is redundant by 1-DoF unless the robot is at a singularity, which occurs only at the workspace limits for this robot.

The null space motion range for a redundant robot depends upon two parameters - the current end-effector pose, and the joint limits. Using the null space projection technique [2], a joint velocity that moves the robot only in null space can be calculated as:

$$\dot{\boldsymbol{q}}_{\text{ns}}(\boldsymbol{q}) = (\boldsymbol{I} - \boldsymbol{J}^{+}(\boldsymbol{q})\,\boldsymbol{J}(\boldsymbol{q}))\,\boldsymbol{\lambda}, \qquad (1)$$

where $\dot{\boldsymbol{q}}_{\text{ns}}$ is the null space joint velocity vector, $\boldsymbol{q}$ is the robot joint position vector, $\boldsymbol{J}(\boldsymbol{q})$ is the Jacobian of the robot, $\boldsymbol{J}^{+}(\boldsymbol{q})$ is the pseudoinverse of the Jacobian, and $\boldsymbol{\lambda}$ is a vector of free parameters. Typically, $\boldsymbol{\lambda}$ is found such that it is optimal for a specified objective.

For our robot, the null space projection matrix, $\boldsymbol{N} = (\boldsymbol{I} - \boldsymbol{J}^{+}(\boldsymbol{q})\,\boldsymbol{J}(\boldsymbol{q}))$, is of rank 1 and it can be characterised completely by the only eigenvector ($\hat{\boldsymbol{e}}_1$) with a non-zero eigenvalue, which can be obtained by normalizing any column of $\boldsymbol{N}$. A joint velocity causing motion only in the null space can be calculated as:

$$\dot{\boldsymbol{q}}_{\text{ns}}(\boldsymbol{q}) = k\,\dot{q}_{\text{max}}\bar{\boldsymbol{e}}_1(\boldsymbol{q}), \quad \bar{\boldsymbol{e}}_1(\boldsymbol{q}) = \frac{\hat{\boldsymbol{e}}_1(\boldsymbol{q})}{\|\hat{\boldsymbol{e}}_1(\boldsymbol{q})\|_\infty}, \qquad (2)$$

where k is a free parameter taken as an input from the user, and $\dot{q}_{\text{max}}$ is a chosen saturation to limit the maximum joint velocity. To decouple the effect of the scale of the Jacobian, we have chosen to normalize $\hat{\mathbf{e}}_1$ with its ℓ^∞ norm, such that the maximum joint velocity of $\dot{\boldsymbol{q}}_{\text{ns}}$ is bounded to $\dot{q}_{\text{max}}$. The velocity calculated for the null space motion is local and is valid only for the current robot configuration ($\boldsymbol{q}$).

In our implementation, the velocity was integrated numerically using Euler's method at every timestep (Δt) to find the different robot configurations within the null space. The limit of null space motion was identified by a violation of any one of the following three conditions.

1. Errors in the end-effector pose of the robot must remain below a chosen threshold: $\Delta x_{\text{max}} = 0.001$ m in position and $\Delta\varphi_{\text{max}} = 0.002$ rad in orientation.
2. The robot joints are within the joint limits.
3. Applicability of linearization of the Jacobian at every timestep was ensured by limiting the change in the current null space velocity vector ($\bar{\boldsymbol{e}}_{1,n}$) with respect to the last timestep ($\bar{\boldsymbol{e}}_{1,n-1}$) and the next timestep estimate ($\tilde{\bar{\boldsymbol{e}}}_{1,n+1}$):

$$\max\left(\text{abs}\left(\bar{\boldsymbol{e}}_{1,n-1} - \bar{\boldsymbol{e}}_{1,n}\right)\right) < \Delta e_{\text{last}}, \text{ and} \qquad (3)$$

$$\max\left(\text{abs}\left(\tilde{\bar{\boldsymbol{e}}}_{1,n+1} - \bar{\boldsymbol{e}}_{1,n}\right)\right) < \Delta e_{\text{next}}. \qquad (4)$$

For the current setup, we chose $\Delta e_{\text{last}} = 0.001$ and $\Delta e_{\text{next}} = 0.1$ and a timestep of $\Delta t = 0.001$ s.

In our setup, the user applies force along the x-axis (f_x) of a 6-DoF ATI Mini45 F/T sensor. The force signal is filtered and saturated changing the value of k between $[-1,1]$, influencing the velocity at which the shape is changed. The maximum joint velocity was saturated with $\dot{q}_{\text{max}} =$ 0.1 rad/s. In this way, the continuous null space movement can be visualized to the user at any end-effector pose (Fig. 2). The test conducted required the user to visualize the null space at different end-effector poses. During this test we observed success/failure of our implementation on a real-time computer at a cycle rate of 1 ms.

III. Results and discussion

The real-time system did not trigger an error or fail during the tests conducted with our implementation. The possible null space configurations were visualized (Fig. 3) while the interface was operated by the user.

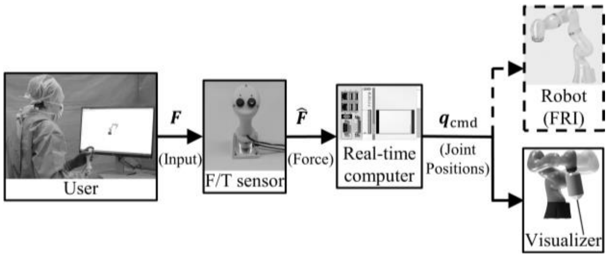

Figure 2: A schematic of the different components of the setup. The interface can be used by a user in the operating room. It measures the force applied using a force/torque (F/T) sensor, which is connected to a Beckhoff real-time system, CX2020. The joint positions in the null space are computed based on the 1-DoF user input and different robot configurations are visualized. Communication to the real robot (dashed line) is part of future work.

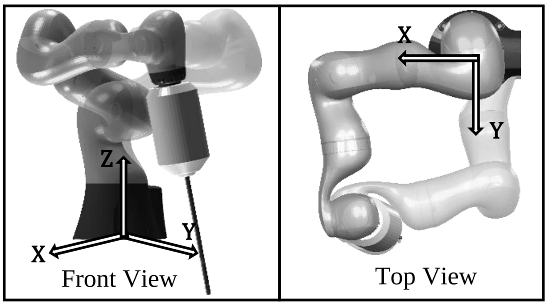

Figure 3: Two different null space configurations visualized as the robot is moved using the interface (the software in [6] is used and adapted for this visualization).

IV. Conclusions

In this work, we present an intuitive interface for a priori visualizing possible null space motion of a redundant robot. This solution enables visualizing the continuous shape change of a robot by a simple user input (force on a joystick) before the motion is executed. Here, we laid the basis for a future integration of our safe and intuitive null space control on a physical KUKA LBR iiwa robot.

Acknowledgments

We gratefully acknowledge funding by the Werner Siemens Foundation through the MIRACLE project and we thank Prof. Dr. med. Niklaus F. Friederich for his continuous support with respect to medical questions.

References

[1] Advanced Osteotomy Tools, *CARLO*, 2017.
[2] B. Siciliano, *Kinematic control of redundant robot manipulators: A tutorial*, Journal of intelligent and robotic systems, vol. 3, 1990, pp. 201-212.
[3] A. Dietrich, C. Ott, A. Albu-Schäffer, *An overview of null space projections for redundant, torque-controlled robots*, The International Journal of Robotics Research, vol. 34, 2015, pp. 1385-1400.
[4] J. Sandoval, H. Su, P. Vieyres, G. Poisson, G. Ferrigno, E. De Momi, *Collaborative framework for robot-assisted minimally invasive surgery using a 7-DOF anthropomorphic robot,* Robotics and Autonomous Systems, vol. 106, 2018, pp. 95-106.
[5] H. Su, C. Yang, G. Ferrigno, E. De Momi, *Improved Human–Robot Collaborative Control of Redundant Robot for Teleoperated Minimally Invasive Surgery*, IEEE Robotics and Automation Letters, vol. 4, 2019, pp. 1447-1453.
[6] Bitbucket repository, *Robot dynamics*, 2016, https://bitbucket.org/leggedrobotics/robotdynamics_exercisse_1a